Bioorganic & Medicinal Chemistry 28 (2020) 115735

Contents lists available at ScienceDirect

Bioorganic & Medicinal Chemistry

journal homepage: www.elsevier.com/locate/bmc

Preparation and evaluation of soluble epoxide hydrolase inhibitors with improved physical properties and potencies for treating diabetic neuropathic pain

Kin Sing Stephen Lee[a,1,2], Jen C. Ng[b], Jun Yang[c], Sung-Hee Hwang[c], Christophe Morisseau[b], Karen Wagner[c], Bruce D. Hammock[a,b,c,*]

[a] Synthia LLC, Davis, CA 95616, United States
[b] Department of Entomology and Nematology, One Shields Ave, University of California-Davis, Davis, CA 95616, United States
[c] EicOsis Human Health, 140 B Street, Suite 5, Number 346, Davis, CA 95616, United States

ARTICLE INFO

Keywords:
Soluble epoxide hydrolase
Inhibitor
Neuropathic pain
Physical properties
Drug target residence time
Drug design

ABSTRACT

Soluble epoxide hydrolase (sEH), a novel therapeutic target for neuropathic pain, is a largely cytosolic enzyme that degrades epoxy-fatty acids (EpFAs), an important class of lipid signaling molecules. Many inhibitors of sEH have been reported, and to date, the 1,3-disubstituted urea has the highest affinity reported for the sEH among the central pharmacophores evaluated. An earlier somewhat water soluble sEH inhibitor taken to the clinic for blood pressure control had mediocre potency (both affinity and kinetics) and a short *in vivo* half-life. We undertook a study to overcome these difficulties, but the sEH inhibitors carrying a 1,3-disubstituted urea often suffer poor physical properties that hinder their formulation. In this report, we described new strategies to improve the physical properties of sEH inhibitors with a 1,3-disubstituted urea while maintaining their potency and drug-target residence time (a complementary *in vitro* parameter) against sEH. To our surprise, we identified two structural modifications that substantially improve the potency and physical properties of sEH inhibitors carrying a 1,3-disubstituted urea pharmacophore. Such improvements will greatly facilitate the movement of sEH inhibitors to the clinic.

1. Introduction

Most diabetic patients will ultimately develop kidney failure, hypertension, stroke and/or other comorbidities. In addition, about 65% of diabetic patients will develop peripheral neuropathy.[1,2] People suffering from diabetic neuropathic pain experience spontaneous pain, hyperalgesia and allodynia which greatly affect the patients' quality of life. It has been suggested that hyperglycemia is the initiating cause of peripheral nerve fiber degeneration which results in pain. However, aggressive glycemic control can only control the progress of neuron degeneration but not reverse the neuropathy.[3] Although semi-effective treatments of diabetic neuropathy are available which include tricyclic antidepressants and selective serotonin reuptake inhibitors, they often have side effects that limit their use. Therefore, alternative therapies with no or greatly reduced side effects are needed. A drug candidate whose action is restricted to peripheral tissues without interference with the CNS effect may also be attractive. Recent studies indicated that soluble epoxide hydrolase (sEH) inhibitors are analgesic in diabetic neuropathic pain models.[4–6] Wagner et al. and Inceoglu et al. have also indicated that the sEH inhibitors are far more efficacious than the clinically approved gabapentin or pregabalin.[7,8]

The sEH (EC 3.3.2.10), which is found in the cytosolic and peroxisomal fractions, is a bifunctional enzyme encoded by the ephx2 gene. The C-terminus domain of sEH, hydrolyzes specific epoxides including bioactive epoxy- fatty acids (EpFAs), to the corresponding 1,2-diols while the *N*-terminal domain has lipid phosphate phosphatase activity.[9] EpFAs, metabolites from the cytochrome P450 (CYP450) pathway within the arachidonic acid cascade, are important lipid mediators.[10] Epoxyeicosatrienoic acids (EETs), epoxyeicosatetraenoic acids, and epoxydocosapentaenoic acids, which are epoxide metabolites of arachidonic acid, eicosapentaenoic acid, and docosahexaenoic acid respectively from CYP450 pathway, have been proven to be anti-inflammatory, vasoregulatory, analgesic, anti-fibrotic and neuroprotective.[9,11–14] Therefore, stabilization of EETs *in vivo* through

* Corresponding author.
[1] Present address: Department of Pharmacology and Toxicology, 1355 Bogue Street, Michigan State University, East Lansing, MI 48824, United States.
[2] Present address: Department of Chemistry, 1355 Bogue Street, Michigan State University, East Lansing, MI 48824, United States.

https://doi.org/10.1016/j.bmc.2020.115735
Received 27 April 2020; Received in revised form 18 August 2020; Accepted 22 August 2020
Available online 31 August 2020
0968-0896/

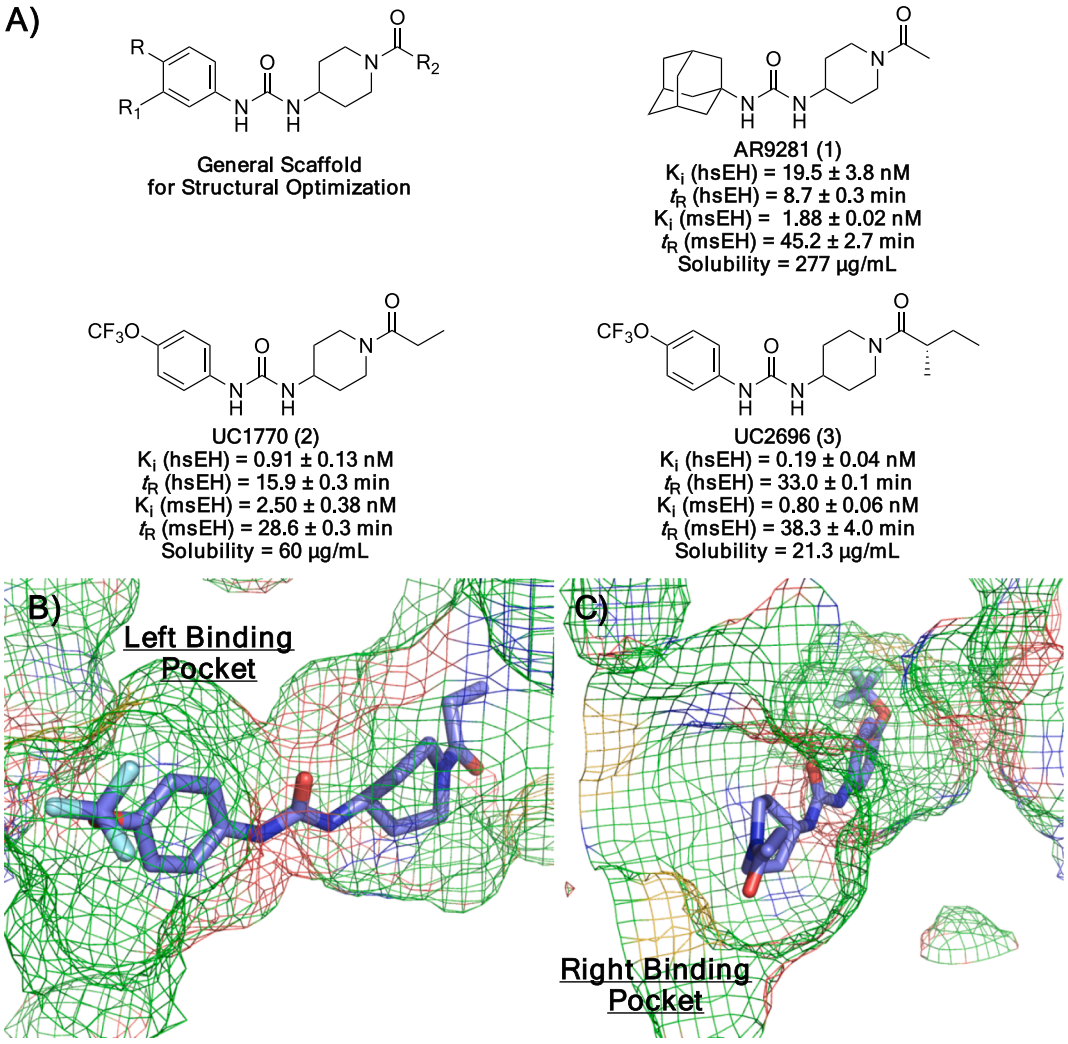

Fig. 1. (A) The general scaffold of the sEH inhibitor being used in this manuscript is shown. AR9281 (APAU or UC1153 labeled (1) was the clinical candidate from Arête Therapeutics. UC1770 is an improved sEH inhibitor widely used by sEH research community. UC2696 (2) is the lead sEH inhibitor for treating diabetic neuropathic pain. (B) The left binding pocket of sEH bound to TPPU (blue) with the structure and direction of the TPPU shown at the bottom of the figure. C) The right binding pocket of sEH bound to TPPU (blue) with the structure and direction of the TPPU shown at the bottom of the figure.

inhibition of sEH is beneficial in many disease states. Thus, sEH is an important pharmaceutical target.[10,15–24]

Over the years, several groups reported the syntheses and the evaluation of sEH inhibitors having different central pharmacophores including but not limited to amides, carbamates, heterocycles, and ureas with potency varying from micromolar to nanomolar ranges.[11,25–34] The 1,3-disubstituted urea is one of the most common and potent central pharmacophores being used to inhibit sEH because the urea makes tight hydrogen bonding with the active residues Try383, Tyr466 and Asp337 and the chemistry is easily accessible.[11,27,29,35,36] However, sEH inhibitors with a 1,3-disubstituted urea often suffer poor solubility and high melting points which hamper the drug formulation needed for high oral availability.[11,29] Unfortunately, structural modifications to improve physical properties including water solubility, logP and melting point have generally resulted in a decrease in potency and less desirable pharmacokinetic properties.[27,28,37,38] Therefore, it is necessary to further optimize the structures to improve their physical properties which can ease the drug formulation processes and improve the oral bioavailability of the sEH inhibitors carrying a 1,3-disubstituted urea as a central pharmacophore. To the best of our knowledge, there is no report of specific modifications that decreases the melting point or improve the solubility of the sEH inhibitors without suffering the loss of potency or bioavailability significantly.[27,35,38,39]

Recent studies suggested that drug-target residence time (t_R), which is a reciprocal of k_{off}, is one of the most important complementary parameters affecting *in vivo* efficacy.[40,41] Inhibitors with long residence times have long durations of action on the enzyme which translates to better and extended *in vivo* efficacy as was shown for sEH inhibitors.[42,43] Recent studies by *Lee et al.* demonstrated that sEH inhibitors with long drug-target residence time will likely have better and extended *in vivo* activity through a phenomenon called target-mediated drug disposition.[43,44] However, the previous clinical candidate of sEH inhibitors: AR9281 (UC1153, from Arête Therapeutics L.L.C.) did not have a good residence time on the recombinant human enzyme, and this in part explains its marginal efficacy in man (Fig. 1).[20,45] Although it had many beneficial properties including surprisingly high water solubility for a urea, low melting point and ease of synthesis, AR9281 (1) also contained an adamantane group used originally to facilitate detection by LC-MS/MS. However, this group leads to rapid cytochrome P450 based metabolism to form complex metabolites, and thus it has a short *in vivo* half-life. Therefore, sEH inhibitors with high potencies and longer drug-residence times (t_R) as well as good pharmacokinetics are essential to engage this pharmaceutical target.

The low potency on the human recombinant enzyme and the other poor properties of AR9281 led to the syntheses of numerous superior sEH inhibitors including UC1770 (**TPPU, inhibitor 2**) which had improved potency on the rodent and different primates sEH, high oral

Table 1
Physical properties and potency of sEH inhibitors with modification of R_2 against human sEH.

No.		Physical Properties					Human sEH	
		Mol. Weight	Sol[a] (pH 7.4) (ug/mL)	Sol[b] (pH 3) (ug/mL)	Melting Point (°C)	logP[c]	Ki (nM)[d]	t_R (min) [d]
3 (2696)	R_2 = 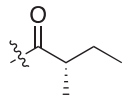	387.40	21.3	N.D.	168.0–169.3 (168.7)	3.97	0.19 ± 0.04	15.9
4	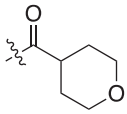	415.11	91	1295	177.4–178.7 (177.9)	3.26	1.43 ± 0.01	20.2
5	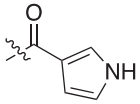	396.14	43	58	131.4–136.1 (133.0)	3.34	0.64 ± 0.17	21.6
6	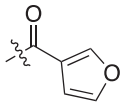	397.12	7.6	26	181.4–184.5 (182.8)	3.63	0.33 ± 0.34	24.5
7	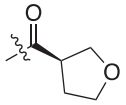	401.16	23	65	180.5–181.7 (180.8)	3.38	1.41 ± 0.11	24.5
8	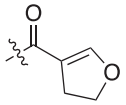	399.14	11	73	190.2–194.7 (192.7)	3.49	0.77 ± 0.02	18.8
9	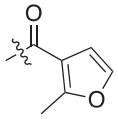	411.14	8.6	7.7	182.5–187.1 (184.8)	4.30	0.55 ± 0.06	21.6
10	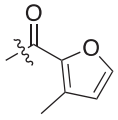	411.14	0.92	3.4	206.2–212.9 (210.4)	4.48	0.26 ± 0.11	30.3
11	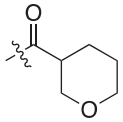	415.17	94	868	176.2–177.7 (177.1)	3.42	1.99 ± 0.23	18.8
12	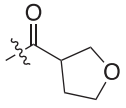	401.16	29	91	163.4–166.3 (164.1)	3.22	1.70 ± 0.01	17.3

[a] Solubility was measured with sodium phosphate buffer (0.1 M, pH 7.4) according to the protocol described by *Lee et al.*[6] and in detail in supporting information. [b] Solubility was measured with sodium phosphate buffer (0.1 M, pH 3.0) according to the protocol described by *Lee et al.*[6] and in detail in supporting information. [c] logP was measured by HPLC method according to *Lee et al.*[6] [d] K_i and t_R, which is a reciprocal of k_{off} was determined by FRET-displacement assay developed by *Lee et al.*[6] The results are the average of duplicates with ± SEM.

availability and good pharmacokinetic properties. Although there was no interest from Arête Therapeutics in developing this compound clinically, it has emerged as the primary tool compound in the filed in spite of challenges in formulating it.

These limitations of AR9281 and TPPU led to the current lead (*S*)-1-(1-(2-methylbutanoyl)piperidin-4-yl)-3-(4-(trifluoromethoxy)phenyl) urea (**2696, inhibitor 3,** Table 1). It is a potent inhibitor (Ki = 0.19 nM) with reasonable drug-target residence time (t_R = 33 min) and good efficacy at 0.3 mg/kg single dose on rodent diabetic neuropathic pain model.[6] However, it suffers poor solubility (21.3 μg/mL) and a relatively high melting point (168.7 °C). Although it is soluble at levels that totally inhibit the target sEH, the combination of poor water solubility, high logP, and high melting point make it difficult to formulate. These difficulties could be addressed by improving the physical properties and/or further improvement in potency. Here, we report the design and synthesis of new sEH inhibitors with dramatically improved physical properties while maintaining or increasing potency and particularly drug-target residence time on sEH. The structural modifications that improved the physical properties and potency of the inhibitors unexpectedly led to compounds with further optimized pharmacokinetic properties and *in vivo* activity as possible clinical candidates.

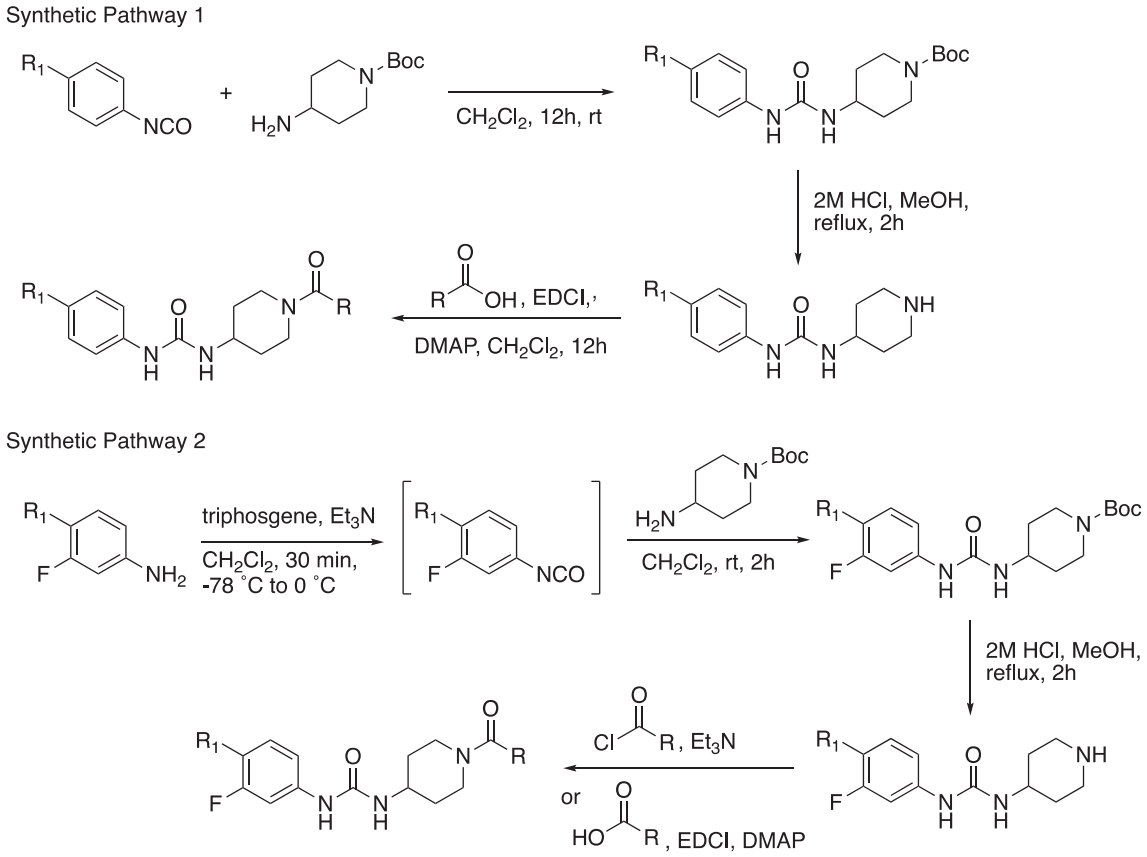

Scheme 1. The syntheses of sEH inhibitors follow two general synthetic pathways depending on the availability of the starting materials.

2. Design principles of new sEH inhibitors with improved physical properties.

The lead candidate (*S*)-1-(1-(2-methylbutanoyl)piperidin-4-yl)-3-(4-(trifluoromethoxy) phenyl)urea (**3**) developed by Hammock's group alleviates nociception responses in a rodent model of diabetic neuropathic pain at low dose (0.3 mg/kg) with high efficacy; however, inhibitor 3 suffers low solubility and the published series with a similar scaffold suffers from high melting points.[6] Thus, the objective was to identify modifications that could enhance the solubility and lower the melting point without hampering the potency of the inhibitors. This is because with highly lipophilic compounds, even a slight improvement in melting point and solubility will significantly ease the formulation processes. Prior research demonstrated that the binding pocket of sEH is promiscuous to a variety of different structures of sEH inhibitors.[6,11,36] In addition, we also showed that the binding pocket is flexible and can accommodate 1,3-disubstituted urea-based inhibitors with different sizes of substituents.[46,47] Based on the crystal structure, the right side of the hydrophobic pocket is relatively large as compared to the left side of the pocket and is more open to the buffer (Fig. 1B, C).[6] Therefore, we first modified the R_2 substituents in order to enhance solubility. Heterocycles are largely employed in the medicinal chemistry to enhance the physical properties of the lead candidates, and we incorporated various heterocycles into the R_2 position of the inhibitors (Fig. 1).

Breaking the symmetry of molecules sometimes disrupts the resulting crystal structure and decreases the melting point.[48] Based on the previous research and the crystal structure, the left side of the binding pocket could accommodate additional substituents on the phenyl group of the inhibitor (Fig. 1B). Here, we tested whether the melting point of inhibitors with the general scaffold as shown in Fig. 1 will be decreased by adding a substituent on the phenyl-group of inhibitor **2** to break the symmetry of this part of the inhibitor.

Finally, all the design and syntheses of new inhibitors were based on our large library of sEH inhibitors using initially murine and human recombinant enzymes and later recombinant enzymes from multiple species to screen for inhibition of the catalytic activity of the epoxide hydrolase. Rapid feedback on inhibitor potency and *in vivo* pharmacokinetics based on our previously developed SAR and computer modeling allowed us to survey multiple series of compounds. The most promising structures are presented here.

3. Result and discussion

3.1. Syntheses of the sEH inhibitors.

The syntheses of majority of sEH inhibitors presented in this report followed our published protocols (Scheme 1**,** please refer to supplemental information for details).[6,35] Briefly, the inhibitors were synthesized by first coupling of the Boc-protected piperidines with the corresponding isocyanates which were either obtained from the commercial sources or prepared *in situ* by triphosgene method with amine. The resulting Boc-protected 1,3-disubstituted ureas were then deprotected with hydrochloric acid. The deprotected 1,3-disubstituted ureas were then coupled with the corresponding acid chloride or carboxylic acid to yield the final product. The resulting inhibitors were then further purified by recrystallization to ensure the high purity of the compounds. The overall yield of the 3 steps synthesis was ranging from 24% to 86% depending on the inhibitors. We attempted to disprove the

Table 2
Physical properties and potency of sEH inhibitors with modification of R_2 against human sEH.

No.		Physical Properties					Human sEH	
		Mol. Weight	Sol[a] (pH 7.4) (ug/mL)	Sol[b] (pH 3) (ug/mL)	Melting Point (°C)	logP [c]	Ki (nM) [d]	t_R (min)[d]
2391 (13)	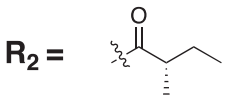	371.40	9.2	N.D.	221.3–225.6 (221.6)	3.84	0.22 ± 0.04	32.2
14	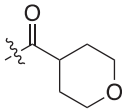	399.18	17.6	61	241.7–243.0 (242.4)	3.16	1.73 ± 0.01	15.9
15	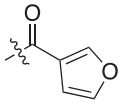	381.13	2.2	6	222.5–223.8 (223.2)	3.50	1.21 ± 0.2	15.9
16	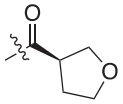	385.16	1.4	58	212.6–218.1 (213.3)	3.27	1.19 ± 0.08	18.8
17	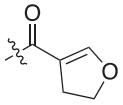	383.15	2.3	8.2	243.0–243.6 (243.2)	3.37	1.03 ± 0.20	11.5
18	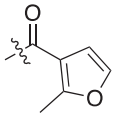	395.15	0.28	2.1	237.3–238.9 (238.0)	4.19	0.51 ± 0.03	15.9
19	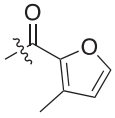	395.15	0.8	1.8	224.9–228.3 (227.2)	4.29	0.22 ± 0.01	15
20	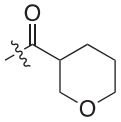	399.18	1.1	25	253.9–255.2 (254.2)	3.41	2.40 ± 0.08	21.6
21	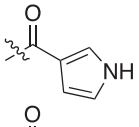	380.15	1.8	13	246.1–248.3 (246.7)	3.26	0.50 ± 0.01	14.4
22	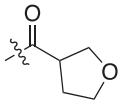	385.16	9.6	50	238.2–239.3 (238.6)	3.16	1.74 ± 0.11	14.4

[a] Solubility was measured with sodium phosphate buffer (0.1 M, pH 7.4) according to the protocol described by *Lee et al.*[6] and in detail in supporting information. [b] Solubility was measured with sodium phosphate buffer (0.1 M, pH 3.0) according to the protocol described by *Lee et al.*[6] and in detail in supporting information. [c] logP was measured by HPLC method according to *Lee et al.*[6] [d] K_i and t_R, which is a reciprocal of k_{off} was determined by FRET-displacement assay developed by *Lee et al.*[6] The results are the average of duplicates with ± SEM.

high purity of the molecules by a variety of techniques including LC-MS with total ion monitoring and UV detection, TLC in multiple systems of F_{254} plates with detection by UV quenching and by charring sprays, melting point, and a variety of spectral methods"

3.2. Specific heterocyclic substituents significantly enhance the solubility of 1,3-disubstituted urea-based sEH inhibitors in an acidic buffer.

We synthesized a new series of sEH inhibitors by incorporating various heterocycles (Table 1) into the R_2 position. Our results indicated that not all the heterocycles incorporated at the R_2 position can enhance the solubility of the inhibitors at pH 7.4 as compared to inhibitor 2 with hydrophobic alkyl group at R_2 (Table 1 and 2). Unlike the other heterocycles, the incorporation of a tetrahydropyran to sEH inhibitors at R_2 (4, 11, 13 and 19) significantly enhances the solubility of sEH inhibitors as compared to inhibitors 3 and 13 (Table 1 and 2). Because these sEH inhibitors are intended for oral administration, we also tested the solubility at acidic pH to ensure the inhibitor remains soluble in the stomach. In general, the solubility of sEH inhibitors with heterocyclic substituents increases under these conditions. Apart from

Table 3
Physical properties and potency of sEH inhibitors with modification of R_3 against human sEH.

No.		Physical Properties				Human sEH	
		Mol. Weight	Sol[a] (pH 7.4) (ug/mL)	Melting Point (°C)	logP [b]	Ki (nM) [c]	t_R (min) [c]
23	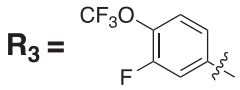	405.39	11	147.0–147.8 (146.2)	5.98	< 0.05	31.7
24	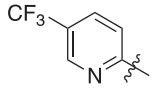	372.39	274	188.5–190.0 (188.8)	3.22	45.0 ± 2.3	5.3
25	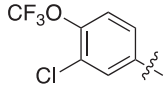	421.85	0.79	183.9–184.5 (184.2)	7.70	3.35 ± 0.42	14.4
26	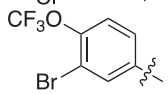	465.29	0.58	197.6–198.5 (198.0)	8.07	3.40 ± 1.38	13.4
27	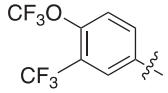	455.40	0.05	201.1–202.1 (201.6)	9.02	9.91 ± 3.37	8.5
28	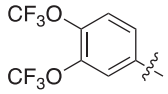	471.40	5.5	170.8–172.4 (171.6)	10.62	9.07 ± 0.36	15.9

[a] Solubility was measured with sodium phosphate buffer (0.1 M, pH 7.4) according to the protocol described by *Lee et al.*[6] and in detail in supporting information. [b] logP was measured by HPLC method according to *Lee et al.*[6] [c] K_i and t_R, which is a reciprocal of k_{off} was determined by FRET-displacement assay developed by *Lee et al.*[6] The results are the average of duplicates with ± SEM.

other heterocycles, sEH inhibitors with a tetrahydropyran at R_2 show an unexpectedly enhanced solubility by at least 10-fold (except 14) at pH 3 and the magnitude of solubility enhancement also was not predicted by the polarity of the heterocyclic substituents in the inhibitors. *Kabli et al.* reported that the saturated heterocycles have higher proton affinity than their corresponding unsaturated heterocycles.[49] In addition, the protonation of the saturated heterocycles occurs at the heteroatoms while the protonation of the unsaturated heterocycles occurs at the alpha-carbon adjacent to the heteroatoms. Therefore, we hypothesize that the proton-heteroatom interaction at the saturated heterocycles under acidic condition improves the solubility of inhibitors carried a tetrahydropyran and a follow up study is underway. The lack of solubility of 1,3-disubstituted ureas is probably due to the formation of insoluble microcrystals in the stomach. Dispersion and enhanced solubility of the tetrahydropyran and related compounds in the stomach could minimize this crystallization.

As we expected, modifications that enhance the solubility of sEH inhibitors usually decrease the potency (both Ki and k_{off}) of the inhibitors. Therefore, the ratio of solubility enhancement over the loss of potency was also analyzed (Table S1). Although the potency of new sEH inhibitors with heterocycles at R_2 generally decreases, the tetrahydropyran substituents provide the best leverage between the solubility, particularly the solubility at acidic pH, and the potency among the other new inhibitors with heterocycles at R_2. In fact, the potency of inhibitor 4 and 11 are still much more potent than the clinical candidate **1** from Arête Therapeutics. The significant enhancement of solubility improves the drug likeness of this series of sEH inhibitors. Because one of the main organs for drug absorption: the stomach, has a pH around 2 to 3, the exceptionally enhanced solubility at pH 3 by the inhibitors with tetrahydropyran improves their absorption and oral bioavailability fulfilling an important need in the area.

3.3. Incorporation of an o-fluorine substituent decreases the melting point of 1,3-disubstituted urea-based inhibitors.

Modifications of the structures of these ureas often have unexpected effects on the melting points of the sEH inhibitors. Previous studies showed that a modification that breaks the symmetry of the molecules generally leads to a decrease in melting point.[6,48] Based on the crystal structure of sEH bound with TPPU, the left-side of the binding pocket can accommodate small substituents on the phenyl- ring (Fig. 1B). It has been reported that a substituent at the 2- position of the phenyl ring (next to the urea) of the inhibitor hampers inhibitor's potency because of the steric hindrance of hydrogen bond formation of a urea proton and the Asp 335 of human sEH.[35] Therefore, we synthesized and tested 6 new inhibitors with modification at the 3- position of the phenyl ring of the inhibitor. Our results (Table 3) indicated that the majority of the substituents tested lead to an increase in melting point and loss of potency by at least 10-fold as compared to inhibitor 3 which indicated that the R groups tested are too large for the binding pocket. However, to our surprise, an addition of fluorine at 3 position of the phenyl group of inhibitor 3 (Table 3, inhibitor 23), decreases the melting point by 22 °C with improved potency. We then further tested whether addition of fluorine at the 3-position of the phenyl ring of this scaffold in general decreases the melting point of sEH inhibitors. Our results (Table 4) indicated that fluorine substitution at the 3-position of the phenyl-group of the inhibitor in general lowers the melting point of the inhibitors. We found that 11 out of 13 inhibitors have melting point at least 9.5 °C (ranging from 9.5 to 35.7 °C) lower than their corresponding inhibitors without the fluorine substitution. While the detailed mechanism on how the fluorine substitution at the 3 position of the phenyl group of the inhibitor lowers the melting point of the inhibitors remains unknown, we hypothesize that such fluorine

Table 4
Physical properties and potency of sEH inhibitors with modification that improves melting point.

No.		Physical Properties				Human sEH		
		Sol[a] (pH 7.4) (ug/mL)	Melting Point (°C)	Melting Point Decrease (°C) [b]	logP [c]	Ki (nM) [d]	Potency Enhancement [e]	t_R (min) [d]
29	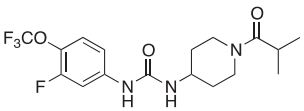	5.3	156.9–157.6 (157.2)	−22.4	4.73	0.31 ± 0.01	1.0	31.7
30	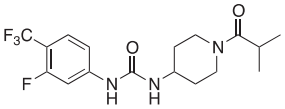	5.9	198.2–200.9 (199.2)	−35.7	4.40	0.49 ± 0.4	1.35	17.3
31	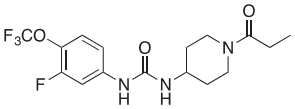	11	172.6–173.1 (172.8)	−26.7	4.00	0.87 ± 0.13	1.05	15.9
32	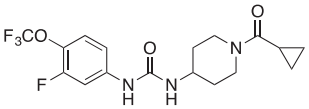	19	178.1–178.9 (178.5)	−15.3	4.19	0.15 ± 0.04	3.67	27.4
33	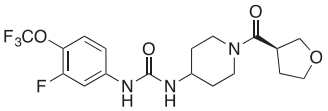	61	168.2–169.7 (168.9)	−11.9	3.59	0.7 ± 0.01	2.1	18.8
34	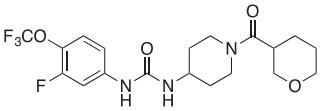	174	158.2–159 (158.4)	−18.7	4.09	0.78 ± 0.19	2.55	17.3
35	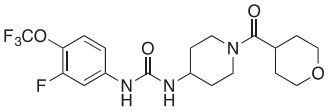	77	172.2–174.0 (173.1)	−4.8	3.73	0.75 ± 0.05	2.31	15.9
36	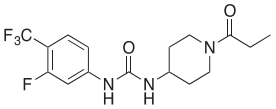	3.9	216.2–216.8 (216.5)	−9.5	3.76	2.94 ± 0.01	1.0	4.8
37	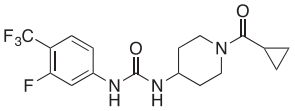	0.46	181.8–182.8 (182.3)	−11.4	3.94	0.38 ± 0.08	1.3	11.8
38	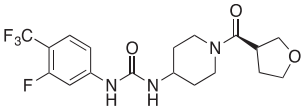	1.9	227.2–229.3 (228.3)	+15	3.41	2.09 ± 0.24	0.57	7.6
39	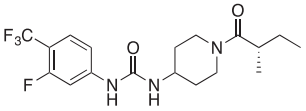	0.46	207.4–208.3 (207.9)	−12.9	5.48	0.37 ± 0.03	0.59	18.8
40	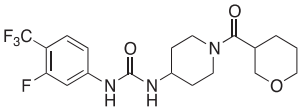	11	236.5–238.3 (237.4)	−16.8	3.84	2.66 ± 0.19	0.90	9.8
41	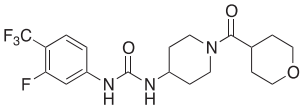	42	219.8–221.8 (220.8)	−21.6	3.52	3.83 ± 0.41	0.45	10.0

[a] Solubility was measured with sodium phosphate buffer (0.1 M, pH 7.4) according to the protocol described by *Lee et al.*[6] and in detail in supporting information. [b] Melting point decrease refer to the melting point changes as compared to the inhibitor without the 3-fluoro substituent on the phenyl ring. Melting point of inhibitor with 3-fluoro substituent on phenyl ring – melting point of the same inhibitor without the 3-fluoro substituent on the phenyl ring. [c] logP was measured by HPLC method according to *Lee et al.*[6] [d] K_i and t_R, which is a reciprocal of k_{off} was determined by FRET-displacement assay developed by *Lee et al.*[6] The results are the average of duplicates with ± SEM. [e] Potency enhancement is the ratio of potency of the inhibitor without 3-fluoro substituent on the phenyl ring over the same inhibitor without 3-fluoro substituent on the phenyl ring.

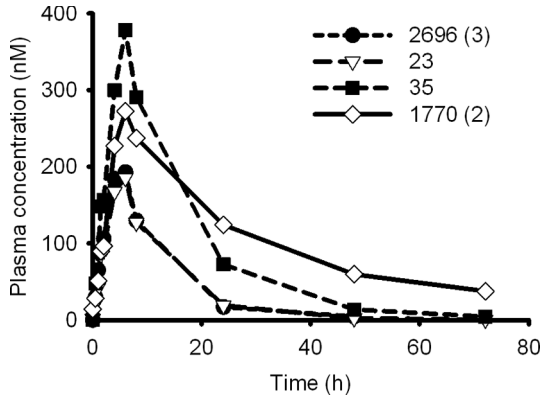

Fig. 2. The PK profile in mice showed that substituent of 4-tetrahydropyran at R_2 (inhibitor 35) or substituent of fluorine at R_1 (inhibitor 23) does not dramatically alter the PK profiles of the sEH inhibitors. The PK profile of 23 is very similar to the PK profile of 2696. Mice (n = 4) were treated by oral dosing with a cassette of 3 to 4 compounds (0.3 mg/kg of each compounds dissolved in 20% PEG400 in oleic acid rich triglycerides). The graphic was prepared by SigmaPlot (SysTat Software, San Jose, CA). The PK profile of 1770 and 2696 was redrawn from *Lee et al.*[6]

substitution can break the overall symmetry of the inhibitors, destabilizing the packing of the molecular crystal.[6,48] In addition, fluorine is much smaller than other substituents tested in Table 4. As a result, the fluorine substitution does not significantly increase the intermolecular Van der Waal's interaction in the packing of the crystal. Thus, it is likely the overall changes of the crystal packing resulting from the fluorine substitution at the 3- position of the phenyl- group of the inhibitor decreases the melting point of the 3-fluorine substituted inhibitor. Besides, our data also indicated that the fluorine substitution at the 3-position of the phenyl group either increases or maintains the potency of the inhibitors. However, an addition of the fluorine sometimes decreases the solubility of the inhibitor. Overall, inhibitors 34 and 35 provide us with better melting points and solubilities. They also yielded good oral availability and pharmacokinetic profiles in murine studies (Fig. 2).

3.4. Further modifications of inhibitor structure failed to yield an inhibitor with better potency and optimized physical properties.

With the encouraging results from the fluorine substitution at the 3-position of the phenyl ring of the inhibitor, we further explored if other modifications in combination with the fluorine at the 3-position would further improve the drug-likeness of the inhibitors. Although the substitution of amide at R_2 position with a carbamate maintains the potency of the inhibitor, this substitution negatively impacts the physical properties (logP, solubility and melting point) of the inhibitors. Because the incorporation of a tetrahydropyran significantly increases the solubility of the inhibitors, particularly at acidic pH 3.0, we installed morpholine at R_2. Replacement of the tetrahydropyran with a morpholine at R_2 results in an inhibitor 49 with similar physical properties and potency as inhibitor 35. Our previous studies indicated that an incorporation of a fluorine at R_2 increases the potency and stability of the inhibitor. Also, an addition of a fluorine may increase the CNS penetration and be beneficial with CNS diseases involving inflammation and endoplasmic reticulum stress.[50,51] Therefore, we incorporated a CF3 group into inhibitor 32 and 37 to create inhibitors 45 and 46. Incorporation of the CF3 group significantly increases the potency of the inhibitor, it also increases the melting point and logP of the inhibitors. Therefore, it was not an ideal modification.

It has also been well-documented that the replacement of a 1,3-disubstituted urea with an amide results sEH inhibitors with significantly improved solubility.[6,35] However, the replacement of the nitrogen at the 1-position of the urea with a carbon leads to a loss of potency by 100-fold, while the replacement of the nitrogen at the 3-position of the urea with a carbon only decreases the potency by 10-fold.[6] Therefore, we synthesized a short series of amide-based inhibitors which the nitrogen at the 3- position of the urea is replaced with a carbon. Our results indicated that the enhancement of the solubility by the amide replacement decreases with an increasing size of the substituent at R_2 (Table 5, inhibitor 42 to 44). Inhibitor 44 resulted in a similar solubility as 23. In addition, as expected, this replacement decreases the potency of the inhibitors significantly. Therefore, we concluded that amide is not a good pharmacophore replacement for the 1,3-disubstituted urea-based sEH inhibitor in our case.

3.5. Pharmacokinetic and in vivo activity evaluation of the selected candidates with improved physical properties.

Based on the *in vitro* data, we selected inhibitors 4, 11, 23, 29, 31, 34 and 35 for PK studies. In general, except for 11 and 34, the selected inhibitors provided good pharmacokinetic profiles at 0.3 mg/kg with good exposure (AUC ≥ 2,500 nM*h and Cmax ≥ 174 nM) and reasonable PK half-life (≥2h) in mouse (Table 6, Table S3). Interestingly, although the physical properties and potencies between sEH inhibitor 4 Vs 11 and inhibitor 34 Vs 35 are similar, the 3-substituted tetrahydropyran substituent seems to show a decreased oral bioavailability as compared to the 4-substituted tetrahydropyran substituent. However, since inhibitors 11 and 35 exist as racemic mixtures, it is possible that one of the enantiomers is less bioavailable. Because the synthesis and characterization of the chiral inhibitors are much more expensive than achiral inhibitors or racemic inhibitors, inhibitor 11 and 35 were not pursued. In addition, the placement of fluorine at the 3- position of the phenyl ring of sEH inhibitors shortened the pharmacokinetic half-life of the inhibitors tested except for compound 35. Such observation may be due to an increase in logP of the compounds which could enhance their metabolism by CYP450s. Our results indicated that both the fluorine substituent at the 3- position of the phenyl ring and 4-substituted tetrahydropyran at R_2 are acceptable replacements to generate new sEH inhibitors with good pharmacokinetic profiles. We have so far not seen undesirable effects of sEH inhibitors attributed to their action in the central nervous system. However, since BBB penetration is not essential for the sEH inhibitors to control peripheral pain in our assays, we concluded to develop inhibitors initially that have low blood brain barrier (BBB) permeability. We used SwissADME to predict BBB penetration based on the BOIL-Egg method.[52] SwissADME predicts that inhibitor 4, 11, 23, 34 and 35 penetrate BBB poorly. Together with the above improvements in physical properties and PK parameters of inhibitors 23 and 35, we felt them suitable to move to pre-clinical toxicological testing. We then tested inhibitor 23 in diabetic animals with a conditioned place preference test, and our results demonstrated that inhibitor 23 relieves pain in diabetic animals similarly to TPPU. The earlier inhibitor 1 (AR9281, UC1153) is a better inhibitor of rodent than human enzymes, resulting in a concern that rodent bioassays will predict greater potency than will be found in the clinic while inhibitor 1 (TPPU, UC1770) has a lower K_i on the human enzyme predicting greater efficacy in man than seen in rodent bioassays. Inhibitor 23 has far greater potency on the human recombinant enzyme than compound 1, and similar potency to compound 2. Thus its biological effects are expected to be similar to compound 2 in rodents as indicated in Fig. 3. Unexpectedly its potency on the human enzyme is exceptionally high leading one to predict the possibility of higher efficacy in the clinic that predicted based on rodent models.

Table 5
Physical properties and potency of sEH inhibitors with modification on R_1, R_2 and N3 against human sEH.

No.		Physical Properties					Human sEH	
		Mol. Weight	Sol[a] (pH 7.4) (ug/mL)	Sol[b] (pH 3) (ug/mL)	Melting Point (°C)	logP [c]	Ki (nM) [d]	t_R (min) [d]
42	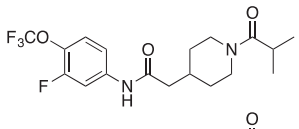	390.38	33	ND	84.2–88.8 (85.0)	5.81	4.72 ± 0.7	4.9
43	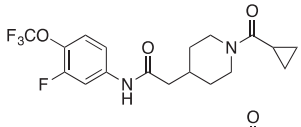	388.36	715	ND	152.3–153.2 (152.8)	5.11	6.60 ± 0.01	4.8
44	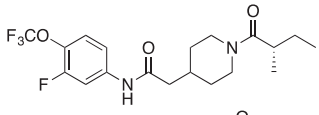	404.41	21	ND	Gel	7.68	3.14 ± 0.70	6.5
45	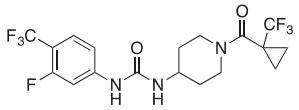	441.35	0.08	ND	240.8–241.7 (241.3)	5.52	0.08 ± 0.01	30.3
46	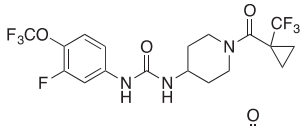	457.35	92	ND	185.4–187 (186.2)	5.94	< 0.05	26.0
47	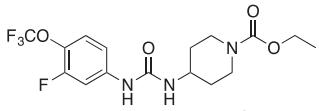	393.34	0.35	ND	182.6–183.0 (182.8)	5.94	< 0.05	26.0
48	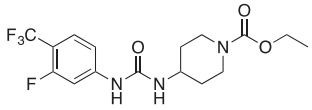	377.34	ND	ND	180.5–181.4 (181.0)	5.46 ± 0.02	0.38 ± 0.03	11.0
49	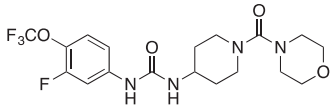	434.39	96	294	160.5–162.6 (161.6)	3.93	0.70 ± 0.06	21.6

[a] Solubility was measured with sodium phosphate buffer (0.1 M, pH 7.4) according to the protocol described by *Lee et al.*[6] and in detail in supporting information. [b] Solubility was measured with sodium phosphate buffer (0.1 M, pH 3.0) according to the protocol described by *Lee et al.*[6] and in detail in supporting information. [c] logP was measured by HPLC method according to *Lee et al.*[6] [d] K_i and t_R, which is a reciprocal of k_{off} was determined by FRET-displacement assay developed by *Lee et al.*[6] The results are the average of duplicates with ± SEM.

In conclusion, we identified two modifications that improved the drug-likeness of the 1,3-disubstituted urea-based sEH inhibitors while maintaining the potency and PK properties of the inhibitors. In this study we identified several compounds with exceptionally slow off rates as indicated by long t_R values of over 30 min (10, 23, 29, 45). These long t_R values do not correspond to logP values and IC_{50} values (not shown here). The incorporation of a tetrahydropyran at R_2 increases the solubility of the inhibitor, particularly at acidic pH which is important for formulation and PK. The addition of a fluorine at the 3-position of the phenyl ring of the inhibitors decreases the melting point of the inhibitors which is a critical parameter when formulating lipophilic materials. The decrease of melting point not only eases the formulation process of drugs but also enhances the oral bioavailability of the drugs in general, and reduces problems with stable polymorphs. Therefore, the improvements made to decrease the melting point to moderate levels are commonly sought after in drug development. Moreover, in this case, an addition of a fluorine at the 3-position of the phenyl ring of the inhibitors maintains or enhances the potency of sEH inhibitors. This is attractive since the PK profiles are similar to the unsubstituted compounds. A combination of both approaches improves several of the inhibitors with several having sub-nanomolar potency on the recombinant human enzyme, adequate water solubility (> 200 μg/mL) and lower melting points. These modifications significantly enhance the drug likeness of the new sEH inhibitors compared to earlier sEH inhibitors with similar activity in relieving pain in diabetic animals and they could be good clinical candidates to treat diabetic neuropathic pain.

Declaration of Competing Interest

The authors declare the following financial interests/personal relationships which may be considered as potential competing interests: [Bruce D. Hammock holds patents on the soluble epoxide hydrolase inhibitors through the University of California and EicOsis. He is a founder and co-owner of Synthia LLC and EicOsis. Jun Yang, Sung-Hee Hwang and Karen Wagner are the employees of EicOsis Human Health which develops soluble epoxide hydrolase inhibitors to treat diabetic neuropathic pain. Kin Sing Stephen Lee holds stock options of EicOsis.].

Table 6
Murine pharmacokinetic parameters, human plasma protein binding (PPB) and BBB penetration prediction of selected sEH inhibitors.

No.	Dose (mg/kg)e	AUC[a] (nM*h)	C_{max}[a] (nM)	$T_{1/2}$[a] (h)	T_{max}[a] (h)	PPB (%)[b]	BBB Penetration Prediction [c]
1[d]	0.5	183	30	3	1	50 ± 2	Yes
2[d]	0.3	10,650	495	12	8	79 ± 1	Yes
3[d]	0.3	2530	195	7.7	4	92.4 ± 0.1	Yes
4	0.3	6371	381	6.3	4.2	94.1 ± 0.4	No
11	0.3	483	38	3.1	6.5	94.1 ± 0.5	No
23	0.3	2169	166	3.3	5.2	99.8 ± 0.1	No
29	0.3	10,893	423	6.6	10	98.7 ± 0.1	Yes
31	0.3	12,982	479	13	6.7	99.2 ± 0.1	Yes
34	0.3	785	112	3.2	2.1	99.4 ± 0.1	No
35	0.3	5557	332	4.3	6.5	98.5 ± 0.1	No

[a] The mice (n = 4) were dosed by oral gavage with a cassette dose of 4 at 0.3 mg/kg (inhibitors were dissolved in 20% PEG400 in oleic acid rich triglycerides). PK parameters of inhibitors were calculated by WinNonlin based on the model of 1 compartment model. [b] The human plasma protein binding was measured at 1 μM inhibitor's concentration using RED Device according to manufacturer's protocol. [c] BBB penetration were predicted by SwissADME based on BOILED-Egg method. [d] These were published by *Lee et al.*[6]

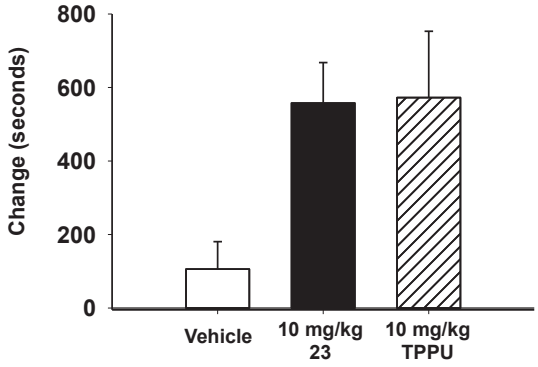

Fig. 3. The conditioned place preference test measures the negative reinforcement of pain relief in a neuropathic animal. The score is the change in time (seconds) spent in the compound paired chamber (preference) after conditioning with the compound to environmental cues. C57B6 male mice induced with streptozocin (n = 7 vehicle, n = 4 5026, n = 6 TPPU).

Acknowledgement

Manuscript preparation was supported by the National Institute of Environmental Health Sciences (NIEHS) R01 ES002710, NIEHS River Award R35 ES030443, and NIEHS Superfund Research Program P42 ES004699 (to B.D.H.) and NIEHS R00 ES024806 (to K.S.S.L). Partial Support came from the National Science Foundation DMS-1761320 (to K.S.S.L). Synthesis and chemical characterization of molecules presented here was carried out at Synthia LLC. Partial support for clinical development of sEH inhibitors comes from the NIEHS SBIR Program R44ES025598, the NIH NINDS Blueprint Neurotherapeutics Network UH2NS094258, National Institute of Neurological Disorders and Stroke (NINDS) U54 NS079202-01 and the National Institutes of Drug Abuse (NIDA) UG3 DA048767.

Appendix A. Supplementary material

Supplementary data to this article can be found online at https://doi.org/10.1016/j.bmc.2020.115735.

References

1. Calcutt NA. Tolerating diabetes: an alternative therapeutic approach for diabetic neuropathy. *Asn Neuro.* 2010;2.
2. Said G. Diabetic neuropathy – a review. *Nature Clin Pract Neurol.* 2007;3:331–340.
3. Veves A, Backonja M, Malik RA. Painful diabetic neuropathy: epidemiology, natural history, early diagnosis, and treatment options. *Pain Med.* 2008;9:660–674.
4. Inceoglu B, Wagner K, Schebb NH, et al. Analgesia mediated by soluble epoxide hydrolase inhibitors is dependent on cAMP. *PNAS.* 2011;108:5093–5097.
5. Wagner K, Yang J, Inceoglu B, Hammock BD. Soluble epoxide hydrolase inhibition is antinociceptive in a mouse model of diabetic neuropathy. *J Pain: Off J Am Pain Soc.* 2014;15:907–914.
6. Lee KS, Liu JY, Wagner KM, et al. Optimized inhibitors of soluble epoxide hydrolase improve in vitro target residence time and in vivo efficacy. *J Med Chem.* 2014;57:7016–7030.
7. Wagner K, Inceoglu B, Dong H, et al. Comparative efficacy of 3 soluble epoxide hydrolase inhibitors in rat neuropathic and inflammatory pain models. *Eur J Pharmacol.* 2013;700:93–101.
8. Inceoglu B, Wagner KM, Yang J, et al. Acute augmentation of epoxygenated fatty acid levels rapidly reduces pain-related behavior in a rat model of type I diabetes. *PNAS.* 2012;109:11390–11395.
9. Morisseau C, Hammock BD. Impact of soluble epoxide hydrolase and epoxyeicosanoids on human health. In: Insel PA, ed., Annual review of pharmacology and toxicology. Vol. 53; 2013. p. 37–58.
10. Spector AA. Arachidonic acid cytochrome P450 epoxygenase pathway. *J Lipid Res.* 2009;50:S52–S56.
11. Shen HC, Hammock BD. Discovery of inhibitors of soluble epoxide hydrolase: a target with multiple potential therapeutic indications. *J Med Chem.* 2012;55:1789–1808.
12. Morisseau C, Inceoglu B, Schmelzer K, et al. Naturally occurring monoepoxides of eicosapentaenoic acid and docosahexaenoic acid are bioactive antihyperalgesic lipids. *J Lipid Res.* 2010;51:3481–3490.
13. Huang HJ, Wang YT, Lin HC, Lee YH, Lin AMY. Soluble epoxide hydrolase inhibition attenuates MPTP-induced neurotoxicity in the nigrostriatal dopaminergic system: involvement of alpha-synuclein aggregation and ER stress. *Mol Neurobiol.* 2018;55:138–144.
14. Kodani SD, Morisseau C. Role of epoxy-fatty acids and epoxide hydrolases in the pathology of neuro-inflammation. *Biochimie.* 2019;159:59–65.
15. Ai D, Pang W, Li N, et al. Soluble epoxide hydrolase plays an essential role in angiotensin II-induced cardiac hypertrophy. *Proc Natl Acad Sci USA.* 2009;106:564–569.
16. Brenneis C, Sisignano M, Coste O, et al. Soluble epoxide hydrolase limits mechanical hyperalgesia during inflammation. *Mol Pain.* 2011;7.
17. Imig JD, Hammock BD. Soluble epoxide hydrolase as a therapeutic target for cardiovascular diseases. *Nat Rev Drug Discovery.* 2009;8:794–805.
18. Inceoglu B, Jinks SL, Schmelzer KR, Waite T, Kim IH, Hammock BD. Inhibition of soluble epoxide hydrolase reduces LPS-induced thermal hyperalgesia and mechanical allodynia in a rat model of inflammatory pain. *Life Sci.* 2006;79:2311–2319.
19. Liu J-Y, Lin Y-P, Qiu H, et al. Substituted phenyl groups improve the pharmacokinetic profile and anti-inflammatory effect of urea-based soluble epoxide hydrolase inhibitors in murine models. *Eur J Pharm Sci.* 2013;48:619–627.
20. Lee KSS, Morisseau C, Yang J, Wang P, Hwang SH, Hammock BD. Forster resonance energy transfer competitive displacement assay for human soluble epoxide hydrolase. *Anal Biochem.* 2013;434:259–268.
21. Schmelzer KR, Kubala L, Newman JW, Kim IH, Eiserich JP, Hammock BD. Soluble epoxide hydrolase is a therapeutic target for acute inflammation. *PNAS.* 2005;102:9772–9777.
22. Ulu A, Harris TR, Morisseau C, et al. Anti-inflammatory effects of omega-3 polyunsaturated fatty acids and soluble epoxide hydrolase inhibitors in angiotensin-II-dependent hypertension. *J Cardiovasc Pharmacol.* 2013;62:285–297.
23. Wagner K, Inceoglu B, Gill SS, Hammock BD. Epoxygenated fatty acids and soluble epoxide hydrolase inhibition: novel mediators of pain reduction. *J Agric Food Chem.* 2011;59:2816–2824.
24. Guedes AGP, Morisseau C, Sole A, et al. Use of a soluble epoxide hydrolase inhibitor as an adjunctive analgesic in a horse with laminitis. *Veterinary Anaesth Analg.* 2013;40:440–448.
25. Eldrup AB, Soleymanzadeh F, Taylor SJ, et al. Structure-Based Optimization Of Arylamides As Inhibitors Of Soluble Epoxide Hydrolase. *J Med Chem.* 2009;52:5880–5895.
26. Huang S-X, Cao B, Morisseau C, Tin Y, Hammock BD, Long Y-Q. Structure-based optimization of the piperazino-containing 1,3-disubstituted ureas affording sub-nanomolar inhibitors of soluble epoxide hydrolase. *Medchemcomm.* 2012;3:379–384.
27. Hwang SH, Tsai H-J, Liu J-Y, Morisseau C, Hammock BD. Orally bioavailable potent soluble epoxide hydrolase inhibitors. *J Med Chem.* 2007;50:3825–3840.
28. Kim I-H, Nishi K, Tsai H-J, et al. Design of bioavailable derivatives of 12-(3-adamantan-1-yl-ureido)dodecanoic acid, a potent inhibitor of the soluble epoxide hydrolase. *Bioorg Med Chem.* 2007;15:312–323.
29. Morisseau C, Goodrow MH, Dowdy D, et al. Potent urea and carbamate inhibitors of soluble epoxide hydrolases. *PNAS.* 1999;96:8849–8854.
30. Podolin PL, Bolognese BJ, Foley JF, et al. In vitro and in vivo characterization of a novel soluble epoxide hydrolase inhibitor. *Prostaglandins Other Lipid Mediat.* 2013;104:25–31.
31. Reema KT, McAtee JJ, Belyanskaya S, et al. Discovery of 1-(1,3,5-triazin-2-yl)piperidine-4-carboxamides as inhibitors of soluble epoxide hydrolase. *Bioorg Med Chem*

Lett. 2013;23:3584–3588.
32. Shen HC, Ding F-X, Deng Q, et al. A strategy of employing aminoheterocycles as amide mimics to identify novel, potent and bioavailable soluble epoxide hydrolase inhibitors. *Bioorg Med Chem Lett.* 2009;19:5716–5721.
33. Shen HC, Ding F-X, Wang S, et al. Discovery of a highly potent, selective, and bioavailable soluble epoxide hydrolase inhibitor with excellent ex vivo target engagement. *J Med Chem.* 2009;52:5009–5012.
34. Tanaka D, Tsuda Y, Shiyama T, et al. A practical use of ligand efficiency indices out of the fragment-based approach: ligand efficiency-guided lead identification of soluble epoxide hydrolase inhibitors. *J Med Chem.* 2011;54:851–857.
35. Rose TE, Morisseau C, Liu J-Y, et al. 1-Aryl-3-(1-acylpiperidin-4-yl)urea inhibitors of human and murine soluble epoxide hydrolase: structure-activity relationships, pharmacokinetics, and reduction of inflammatory pain. *J Med Chem.* 2010;53:7067–7075.
36. Kim I-H, Tsai H-J, Nishi K, Kasagami T, Morisseau C, Hammock BD. 1,3-disubstituted ureas functionalized with ether groups are potent inhibitors of the soluble epoxide hydrolase with improved pharmacokinetic properties. *J Med Chem.* 2007;50:5217–5226.
37. Liu JY, Tsai HJ, Hwang SH, Jones PD, Morisseau C, Hammock BD. Pharmacokinetic optimization of four soluble epoxide hydrolase inhibitors for use in a murine model of inflammation. *Br J Pharmacol.* 2009;156:284–296.
38. Jones PD, Tsai HJ, Do ZN, Morisseau C, Hammock BD. Synthesis and SAR of conformationally restricted inhibitors of soluble epoxide hydrolase. *Bioorg Med Chem Lett.* 2006;16:5212–5216.
39. Tsai H-J, Hwang SH, Morisseau C, et al. Pharmacokinetic screening of soluble epoxide hydrolase inhibitors in dogs. *Eur J Pharm Sci.* 2010;40:222–238.
40. Dahl G, Akerud T. Pharmacokinetics and the drug-target residence time concept. *Drug Discovery Today.* 2013;18:697–707.
41. Copeland RA. Drug-target interaction kinetics: underutilized in drug optimization? *Future Med Chem.* 2016;8:2173–2175.
42. Copeland RA, Pompliano DL, Meek TD. Opinion – Drug-target residence time and its implications for lead optimization. *Nat Rev Drug Discovery.* 2006;5:730–739.
43. Lee KSS, Yang J, Niu J, et al. Drug-target residence time affects in vivo target occupancy through multiple pathways. *ACS Cent Sci.* 2019;5:1614–1624.
44. Wu N, Hammock B, Lee KSS, An G. Simultaneous Target-Mediated Drug Disposition (TMDD) model for two small-molecule compounds competing for their pharmacological target: soluble epoxide hydrolase. *J Pharmacol Exp Therap.* 2020.
45. Chen D, Whitcomb R, MacIntyre E, et al. Pharmacokinetics and pharmacodynamics of AR9281, an inhibitor of soluble epoxide hydrolase, in single- and multiple-dose studies in healthy human subjects. *J Clin Pharmacol.* 2012;52:319–328.
46. Burmistrov V, Morisseau C, Harris TR, Butov G, Hammock BD. Effects of adamantane alterations on soluble epoxide hydrolase inhibition potency, physical properties and metabolic stability. *Bioorg Chem.* 2018;76:510–527.
47. Lee KS, Henriksen NM, Ng CJ, et al. Probing the orientation of inhibitor and epoxyeicosatrienoic acid binding in the active site of soluble epoxide hydrolase. *Arch Biochem Biophys.* 2017;613:1–11.
48. Pinal R. Effect of molecular symmetry on melting temperature and solubility. *Org Biomol Chem.* 2004;2:2692–2699.
49. Kabli S, van Beelen ESE, Ingemann S, Henriksen L, Hammerum S. The proton affinities of saturated and unsaturated heterocyclic molecules. *Int J Mass Spectrom.* 2006;249–250:370–378.
50. Ren Q, Ma M, Ishima T, et al. Gene deficiency and pharmacological inhibition of soluble epoxide hydrolase confers resilience to repeated social defeat stress. *Proc Natl Acad Sci.* 2016;113:E1944.
51. Ren Q, Ma M, Yang J, et al. Soluble epoxide hydrolase plays a key role in the pathogenesis of Parkinson's disease. *PNAS.* 2018;115:E5815–E5823.
52. Daina A, Zoete V. A BOILED-egg to predict gastrointestinal absorption and brain penetration of small molecules. *ChemMedChem.* 2016;11:1117–1121.